Thin Solid Films 518 (2010) 1682–1688

Contents lists available at ScienceDirect

Thin Solid Films

journal homepage: www.elsevier.com/locate/tsf

Changes in Gd_2O_3 films grown on Si(100) as a function of nitridation temperature and Zr incorporation

W.J. Lee [a], M.-H. Cho [a,*], Y.K. Kim [a], J.H. Baeck [a], I.S. Jeong [a], K. Jeong [a], K.B. Chung [b], S.Y. Kim [c], D.-H. Ko [c]

[a] Department of Physics and Applied Physics, Yonsei University, Seoul 120-749, Republic of Korea
[b] Department of Physics, Dankook University, Dongnamgu Anseodong 29, Cheonan 330-714, Republic of Korea
[c] Department of Material Science and Engineering, Yonsei University, Seoul 120-749, Republic of Korea

ARTICLE INFO

Article history:
Received 4 February 2009
Received in revised form 12 November 2009
Accepted 20 November 2009
Available online 29 November 2009

PACS:
77.55.+f
71.20.Eh
68.55.Jk

Keywords:
Gadolinium oxide
Annealing
Ammonia
Nitridation
Silicides
Zr-silicate
Interfacial reactions
X-ray diffraction
X-ray photoelectron spectroscopy
Near edge X-ray absorption spectroscopy

ABSTRACT

We investigated Gd_2O_3 and Zr-incorporated Gd_2O_3 films grown on Si (100) as a function of nitridation temperature under an NH_3 ambient and the incorporation of Zr into the film. The formation of a silicide layer at the interfacial region was suppressed in cases of Zr-incorporated or NH_3-nitried Gd_2O_3 films. The crystalline structure was affected when zirconium, with a relatively small ionic radius, was substituted with gadolinium. When the concentration of Zr atoms in a Gd_2O_3 film reaches a specific level ($Gd_{0.6}Zr_{1.9}O_{4.3}$), phase transition occurred from cubic Gd_2O_3 to monoclinic ZrO_2. However, the monoclinic phase disappeared after nitridation at 900 °C in an NH_3 ambient. The majority of the nitrogen atoms accumulated near the interface in the films and the concentration of incorporated N increased with increasing Zr content and NH_3 annealing temperature. Moreover, nitrogen atoms bonded to Zr-silicate at the interface, in preference to ZrO_2 in the film. These incorporation characteristics of nitrogen into Zr-incorporated Gd_2O_3 film have an effect on the thermal stability and crystalline structure of a film.

1. Introduction

As device size continues to be scaled down, the gate dielectric layer in complementary metal-oxide-semiconductors has nearly approached its thickness limit because of excess gate leakage current and poor reliability issues. In particular, direct-tunneling current is closely dependent on the oxide thickness, an important variable in terms of the reliability of transistors. Because high-k oxides allow a physically thicker layer to be produced with the same capacitance that is required for the conventional gate dielectric layer of SiO_2, a high dielectric constant (k) oxide is generally thought to be an alternative gate dielectric material. To replace conventional SiO_2, which has a high dielectric oxide, various requirements need to be satisfied; permittivity, band gap, thermodynamic stability, interface quality and reliability etc [1]. Among the possible high dielectric materials, HfO_2, ZrO_2, and their silicates are currently viewed as attractive candidates, because their dielectric constants are appropriate for effectively reducing leakage current [2,3]. Rare-earth materials with a high dielectric constant are also considered to be promising candidates. Among the rare-earth materials, Gd_2O_3 has a sufficiently high dielectric constant ($k \sim 16$), which is a reasonable value for it to be used as an alternative gate dielectric [4,5]. Moreover, the lattice constant of cubic Gd_2O_3 ($a = 10.812$ Å) nearly matches twice the silicon lattice constant ($2a = 10.862$ Å), which is an advantageous feature that could reduce interfacial strain between an oxide film and a silicon substrate. The Gd_2O_3 film as a gate oxide, among the various high-k materials, is the first insulating material to be successfully fabricated into GaAs MOSFETs [6].

Gadolinium readily reacts with oxygen and forms an oxide layer, due to a low Gibbs free energy ($\Delta G \sim -1539$ kJ/mol) at ~730 °C [7]. However, since the reaction temperature between gadolinium and silicon is lower than that of gadolinium and oxygen, the formation of a Gd-silicide layer is inevitable on a Si substrate. The formation of a Gd-silicide layer degrades certain oxide qualities, such as stoichiometry and crystallinity, which can result in a leakage source or a leakage current path into the gate oxide of MOS devices. This leads to

* Corresponding author.
E-mail address: mh.cho@yonsei.ac.kr (M.-H. Cho).

0040-6090/$ – see front matter © 2009 Elsevier B.V. All rights reserved.
doi:10.1016/j.tsf.2009.11.071

undesirable results related to the degradation of structure stability and deterioration of device performance at high temperatures.

On the other hand, when ZrO_2 is incorporated into a Gd_2O_3 film, the film becomes thermodynamically stable when in contact with Si, and has a wide band gap (5.1–7.8 eV) [8]. Such ZrO_2–Si band offsets would be predicted to be favorable for blocking both holes and electrons [9]. Our previous studies also reported that, in the case of the incorporation of Zr into Gd_2O_3 films deposited on Si (111), interfacial layer formation was suppressed and crystal quality was enhanced, compared with that of as-grown Gd_2O_3 films; i.e., the incorporated ZrO_2 can control the interfacial layer of Gd_2O_3 [10,11]. We describe herein our attempts to improve the enhanced Gd_2O_3/Si(100) interfacial quality by incorporating ZrO_2 into the Gd_2O_3 films and to better understand interfacial interactions between an oxide film and a Si substrate, so as to control the interfacial layer and film quality.

The focus of this work was on the characteristics of NH_3-nitridied Gd_2O_3 films in the case of both as-grown films and Zr-incorporated films. It is well known that theNH_3-nitridation treatment has some advantages; interfacial reactions are suppressed, thermal stability is improved, dopant diffusion is decreased, and the electrical characteristics of the film are enhanced [12,13]. Moreover, NH_3-nitridation results in an increased dielectric constant and resistance impurity while it introduces a large number of traps in the film [14,15]. Studies on the complementary properties of nitrided Gd_2O_3 and ZrO_2 could offer the potential for applications devices. We focused on the investigation of physical properties such as crystalline structure, chemical bonding at the interface and electronic structure because it is important to understand the reactions between an oxide film and a silicon substrate in more detail.

2. Experiments

P-type (100) oriented Si wafers are cleaned using the Standard Radio Corporation of America (RCA) method [16]. The solution consists of a 1:1:5 mixture of NH_4OH, H_2O_2 and H_2O at 80 °C and is an effective decontaminant with an acceptable level of damage to the surface of the bulk silicon. A 1:1:6 solution of $HCl:H_2O_2:H_2O$ heated to 80 °C was used to remove extraneous metal ions. The RCA cleaning resulted in 4–6 layers of SiO_2 while removing organic and metallic residues from the surface. After removing the growing SiO_2 layers on cleaned Si wafer by treatment with a dilute solution of HF, the sample was transferred to a growth chamber with a base pressure 5×10^{-9} Torr. Gd_2O_3 was deposited by means of a k-cell effusion method and zirconium was evaporated by electron beam evaporation in order to incorporate zirconium into the Gd_2O_3 film. The deposition rate for Gd_2O_3 and ZrO_2 was controlled from ~0.03 Å/s to 0.4 Å/s and from 0.00 Å/s to 0.1 Å/s, respectively. The partial pressure of oxygen and substrate temperature was maintained at 2.0×10^{-6} Torr and 700 °C, respectively, during the deposition of the films on Si(100). A NH_3-nitridation treatment was performed on the grown films at annealing temperatures of 700 °C, 800 °C and 900 °C for 1 min using a rapid thermal processing system. Electronic and crystalline structures of the samples with various thicknesses of 2 nm, 4 nm and 30 nm were characterized using X-ray photoelectron spectroscopy (XPS), near edge X-ray absorption spectroscopy (NEXAFS), and X-ray diffraction (XRD). The chemical composition and the binding states of the Zr-incorporated Gd_2O_3 films treated by nitridation annealing were characterized by XPS. The binding energy was calibrated with reference to the bulk Si peak at 99.2 eV. NEXAFS experiments provided the change in the electronic structure, which was related to the change in the crystalline structure of the film depending on the quantity of the Zr content incorporated into the film. O K-edge of photon-absorption spectra were collected at normal incidence with a photodiode using the synchrotron U7 beam line at the Pohang light source. XRD spectra were obtained using a Philips diffractometer with CuKα radiation (wavelength: 1.5406) to determine the crystal structure of the Gd_2O_3 films as a function of the incorporated Zr content.

3. Results and discussion

Fig. 1 shows the change in XRD patterns of as-grown Gd_2O_3 films and corresponding nitrided films grown on Si (100) as a function of incorporated Zr content. The composition of the Zr-incorporated Gd_2O_3 films was determined by RBS measurements: i.e., the stoichiometry of these films was determined to be $Gd_2O_{3.2}$, $Gd_2Zr_{0.3}O_{3.5}$, $Gd_2Zr_{1.3}O_{4.5}$, and $Gd_{0.6}Zr_{1.9}O_{4.5}$ by RUMP simulation of the random RBS spectrum. The measured lattice parameter of the Gd_2O_3 (10.82 Å), obtained using XRD, is in agreement with that of bulk (10.812 Å) from the calculated value of the lattice parameter. The crystalline structure of the grown film shows a poly crystalline structure with growth directions of Gd_2O_3 (222), Gd_2O_3 (440), and $GdSi_2$ (004). The preferred growth direction of Gd_2O_3 (440) and the formation of a Gd-silicide layer has already been reported [17,18]. In Fig. 1(a) an as-grown Gd_2O_3 film grown on Si (100) exhibits preferred (440), (400) peaks and an imperceptible (222) peak. Gd_2O_3 belonging to space group Ia3 is an isomorphic structure of Mn_2O_3, which prefers a (110) direction growth on the (100) surface [18]. The peak observed at 33° is caused by the structure of Si (200) and cubic Gd_2O_3 (400), which is indicative of a cube-on-cube growth on Si (100)

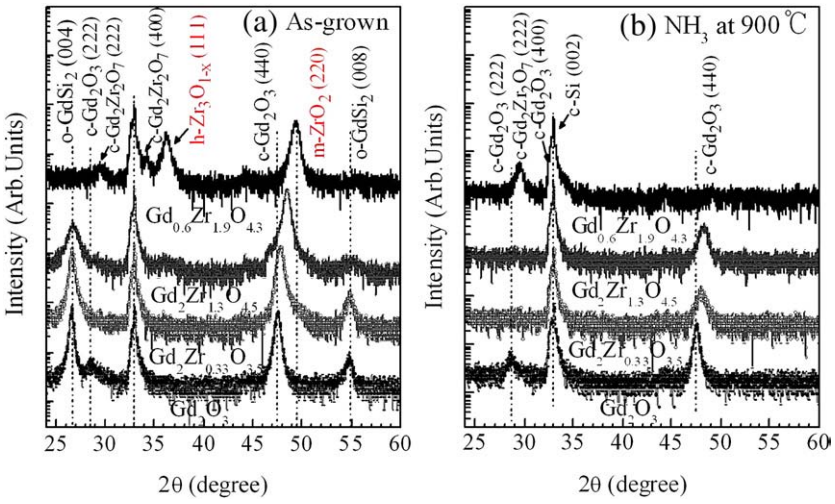

Fig. 1. XRD patterns (θ–2θ scan) of Gd_2O_3 and Zr-incorporated Gd_2O_3 films (30 nm) grown on Si(100) as a function of zirconium content (a) without any nitridation process and (b) with NH_3 nitridation at 900 °C. (c: cubic, m: monoclinic, h: hexagonal, and o: orthorhombic phase).

substrate. Moreover, orthorhombic $GdSi_2$ (l00) silicide peaks indicate that interfacial reactions are occurring easily between gadolinium and the silicon substrate [19,20]. However, as the Zr concentration incorporated into the Gd_2O_3 film increases, these XRD patterns gradually changed: i.e., both the $GdSi_2$ (l00) and weak cubic Gd_2O_3 (222) peaks are suppressed, while the cubic Gd_2O_3 (440) peak shifted toward higher 2θ. When Zr atoms in a Gd_2O_3 film reach a specific level ($Gd_{0.6}Zr_{1.9}O_{4.3}$), the crystalline structure of the Gd_2O_3 film undergoes a drastic change: i.e., at this composition, the Gd-silicide peaks completely disappear, while cubic $Gd_2Zr_2O_7$ (222), (400) appears for the first time. Moreover, a phase transition, from cubic Gd_2O_3 (440) to monoclinic ZrO_2 (220), occurred. The emerging hexagonal Zr_3O_{1-x} (111) and monoclinic ZrO_2 peaks at 36.2° and 49.4°, respectively, indicate that a ZrO_2 phase was partially formed in the films. Based on reported data, the growth of a metal oxide such as Gd_2O_3 starts with nucleation at many different sites across the substrate surface. When Zr atoms are introduced into the film, they occupy reaction sites in preference to Gd, due to their rapid diffusivity and subsequently form networks with Si at the interface during the initial stage [20]. Therefore, the results indicate that competition for the growth direction and phase transition along with the quantity of Zr incorporated into Gd_2O_3 films occurred during the initial phase of growth. The effect on the process at the interface may be gradually increased as the quantity of incorporated Zr increases. Thus, Zr incorporation into a Gd_2O_3 film impedes the growth of the Gd-silicide layer at the interface as they substitute for Gd sites in the unit cell. Moreover, an increased level of Zr atoms in the films can cause shrinkage of the lattice constant because the ionic radius of Zr is smaller than that of Gd [21]. In particular, when the composition of the film is Zr-rich ($Gd_{0.6}Zr_{1.9}O_{4.3}$), monoclinic-ZrO_2, hexagonal-Zr_3O_{1-x} peaks, and cubic-$Gd_2Zr_2O_7$ peaks appear. From the structural point of view, the findings suggest that a specific stoichiometry exists, where both phases of ZrO_2 and Gd_2O_3 are able to coexist in the films. Furthermore, the low intensity of the $Gd_2Zr_2O_7$ peaks indicate the existence of Gd-Zr-O networking in the film and the hexagonal Zr_3O_{1-x} peak is thought to be the result of an oxygen deficiency at the interface region. Fig. 1(b) shows XRD spectra of the annealed films at 900 °C in an NH_3 ambient. Similar tendency was also observed in the nitride film at 700 °C and 800 °C. Compared with Fig. 1(a), the Gd-silicide peaks of an as-grown Gd_2O_3 film were rapidly impeded in the nitride film, while the c-Gd_2O_3 (400) and (440) peaks were still maintained in Fig. 1(b). As the level of Zr incorporated into the Gd_2O_3 films increased, c-Gd_2O_3 (222) disappears and the intensity of c-Gd_2O_3 (440) is gradually lowered. An interesting finding related to these changes is that when the quantity of Zr reaches $Gd_{0.6}Zr_{1.9}O_{4.3}$, the m-ZrO_2 and h-Zr_3O_{1-x} peaks disappeared, and only the $Gd_2Zr_2O_7$ (222) peak was present, indicating that the crystalline structure was altered as the result of the NH_3-nitridation at a high temperature at 900 °C. In general, bulk ZrO_2 has three crystal structures—monoclinic (<1170 °C), tetragonal (1170 °C–2300 °C) and cubic phases (2300 °C–2680 °C), while the phase of a ZrO_2 film depends on thickness and temperature [22]. In our system, the high Zr

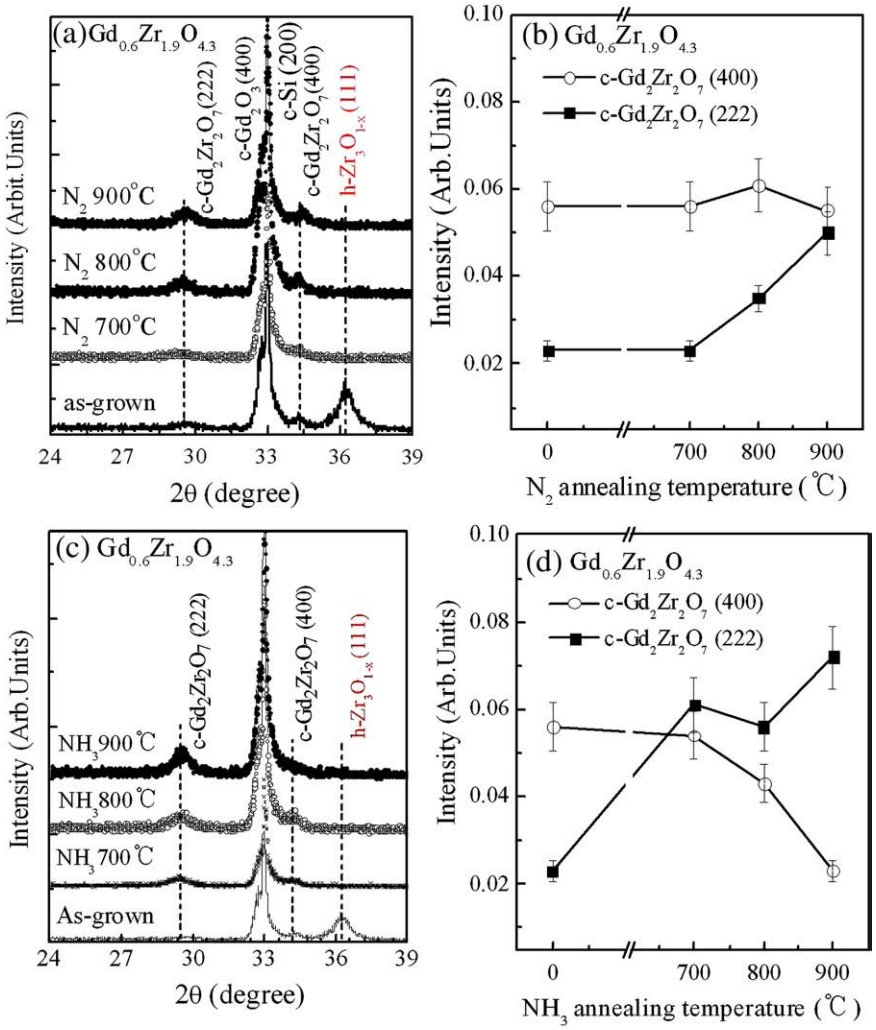

Fig. 2. XRD patterns (θ–2θ scan) of as-grown $Gd_{0.6}Zr_{1.9}O_{4.3}$ film (30 nm) as a function of annealing temperature of 700 °C, 800 °C, and 900 °C (a) in ambient of N_2, (c) and NH_3. For the $Gd_{0.6}Zr_{1.9}O_{4.3}$ film (30 nm), the intensity of c-$Gd_2Zr_2O_7$(400) and c-$Gd_2Zr_2O_7$(222) at annealing temperatures of 700 °C, 800 °C, and 900 °C (b) in ambient of N_2, (d) and NH_3. (c-$Gd_2Zr_2O_7$(400): circle shape, c-$Gd_2Zr_2O_7$(222): rectangular shape).

incorporation into the Gd_2O_3 film assisted in the growth of monoclinic ZrO_2 while NH_3-nitridation inhibited the formation of monoclinic ZrO_2.

Since a $Gd_{0.6}Zr_{1.9}O_{4.3}$ film that contains large amounts of Zr has a different crystalline structure from that of the other films that contain relatively lower quantities of Zr, we examined changes in their XRD peaks within the range from 25° to 40° in detail, as a function of both N_2 and NH_3 annealing temperature, as shown in Fig. 2. We observed that the c-Gd_2O_3 (400) peak was retained in Gd_2O_3 films that contained incorporated Zr, as well as samples that had been annealed at a high temperature, which is due to a high solubility of solid ZrO_2 in Gd_2O_3 at temperatures in excess of ~730 °C [23]. This phenomenon also can be attributed to epitaxially growing rare-earth oxides on Si, because the direction of growth is determined by the underlying surface state of the Si substrate, the relationship for which has been reported to be as follows; Gd_2O_3(111)/Si(111) and Gd_2O_3[110]/Si[110] [10,11]. Furthermore, the emerging hexagonal Zr_3O_{1-x}(111) peak in the as-grown $Gd_{0.6}Zr_{1.9}O_{4.3}$ film disappeared during both the N_2 and NH_3 annealing processes, indicating that Zr_3O_{1-x} is in an unstable state at high temperatures. We can thus conclude that the (100) growth direction becomes predominant for the Si (100) substrate, resulting in the formation of c-Gd_2O_3 (400) and c-$Gd_2Zr_2O_7$ (400). When Zr is properly incorporated into a Gd_2O_3 film, it plays an important role in enhancing the crystalline structure by the lowering oxygen activation barrier, while an excessive supply of Zr atoms induces $Gd_2Zr_2O_7$ bonding in the films. In the phase diagram of Gd_2O_3–ZrO_2, $Gd_2Zr_2O_7$ is present as a cubic pyrochlore phase at temperatures of about 1000 °C. In our experiments, the $Gd_2Zr_2O_7$ structure with two growth directions (222) and (400) at 29.480° and 34.224°, respectively, emerged when the stoichiometry was specifically $Gd_{0.6}Zr_{1.9}O_{4.3}$. When the annealing temperature was increased, we observed that their peak intensities were dependent on the annealing ambient; i.e., the change in the peak intensity is slight under the N_2 ambient, as shown in Fig. 2(a), while it clearly increases with increasing annealing temperature increased under the NH_3 ambient in Fig. 2(c). The difference in the peak change under both N_2 and NH_3 ambient can be represented more clearly by normalization of XRD pattern as a function of annealing temperature from Fig. 2(a) and (c) when expressed as the symbol shown in Fig. 2(b) and (d). From these data, we conclude that growth in the (111) direction dominates the crystalline structure for the case of a composition of $Gd_{0.6}Zr_{1.9}O_{4.3}$ as the annealing temperature increases under both N_2 and NH_3 ambient, while the (100) direction is suppressed under an NH_3 ambient. Thus, the film becomes a single phase when it is grown depending on the NH_3 annealing temperature, which permits the incorporation of N into the $Gd_{0.6}Zr_{1.9}O_{4.3}$ film.

Angle-resolved X-ray photoemission spectroscopy (ARXPS) was employed to determine the distribution of incorporated nitrogen within the Gd_2O_3 and in the Zr-incorporated Gd_2O_3 film as shown in Fig. 3(a)–(c). The data show that N is incorporated to a high degree at the interface during the nitridation process in the NH_3 ambient. During the nitridation process at high temperature, NH_3 molecules generally decompose into nitrogen and hydrogen at temperatures over 450 °C and hydrogen atoms are then desorbed from the film at temperatures of about 500 °C [24]. The decomposed nitrogen atoms are inter-diffused into the film and react with the Si substrate, resulting in the formation of silicon nitride near the interface region. The XPS data for N 1s clearly shows that Gd_2O_3 without any Zr content possesses a low level of nitrogen, while the Zr-incorporated Gd_2O_3 film contains significantly high nitrogen content with nitridation temperature, as shown in Fig. 3. Moreover, the dependence of the take-off angle on the intensity of the nitrogen peak indicates that nitrogen primarily accumulates near the interface between the oxide film and substrate, rather than near the surface. Many interesting conclusions can be arrived at, from detailed examinations of XPS data, as follows. First, Zr atoms, when added to Gd_2O_3 films, play an important role in attracting nitrogen to the oxide films, compared to the amount of N in films that contain no incorporated Zr. Second,

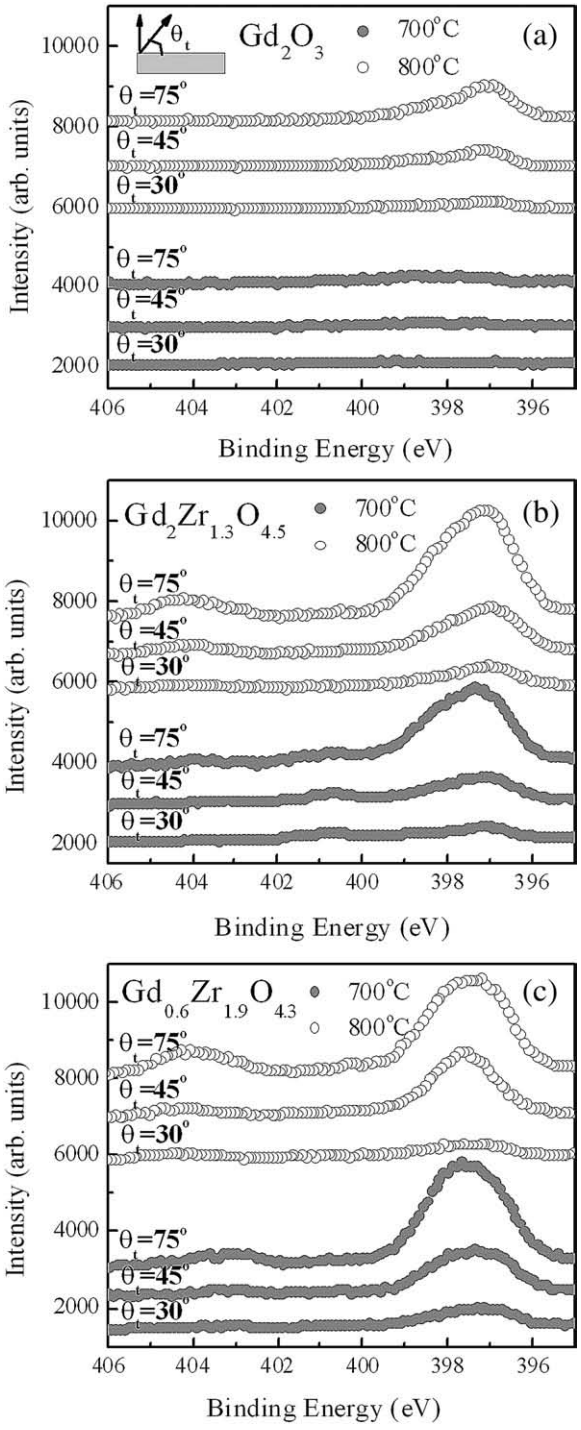

Fig. 3. N 1s ARXPS spectra taken at various take-off angles (75°, 45°, and 30°) for various compositions of (a) as-grown Gd_2O_3, (b) $Gd_2Zr_{1.3}O_{4.5}$, and (c) $Gd_{0.6}Zr_{1.9}O_{4.3}$ films as a function of nitridation temperature in an ambient of NH_3 at 700 °C and 800 °C, respectively. (Thickness of each film: 4 nm).

molecular N_2 is adsorbed near the interface at a binding energy of 404 eV. The role of Zr can be explained by replacing Gd with Zr, which suppresses Gd-silicide formation. Thus, the suppression of interfacial reactions indicates that the interfacial state is significantly different between a film with and without Zr. During the nitridation process, residual oxygen reacts with the interfacial layer, resulting in the formation of a silicate layer, as shown in Fig. 4. The Si 2p peak consists of three peaks that can be assigned to bulk Si (99.2 eV), silicate (~102 eV), and dioxide (~103 eV). In cases of as-grown oxide films,

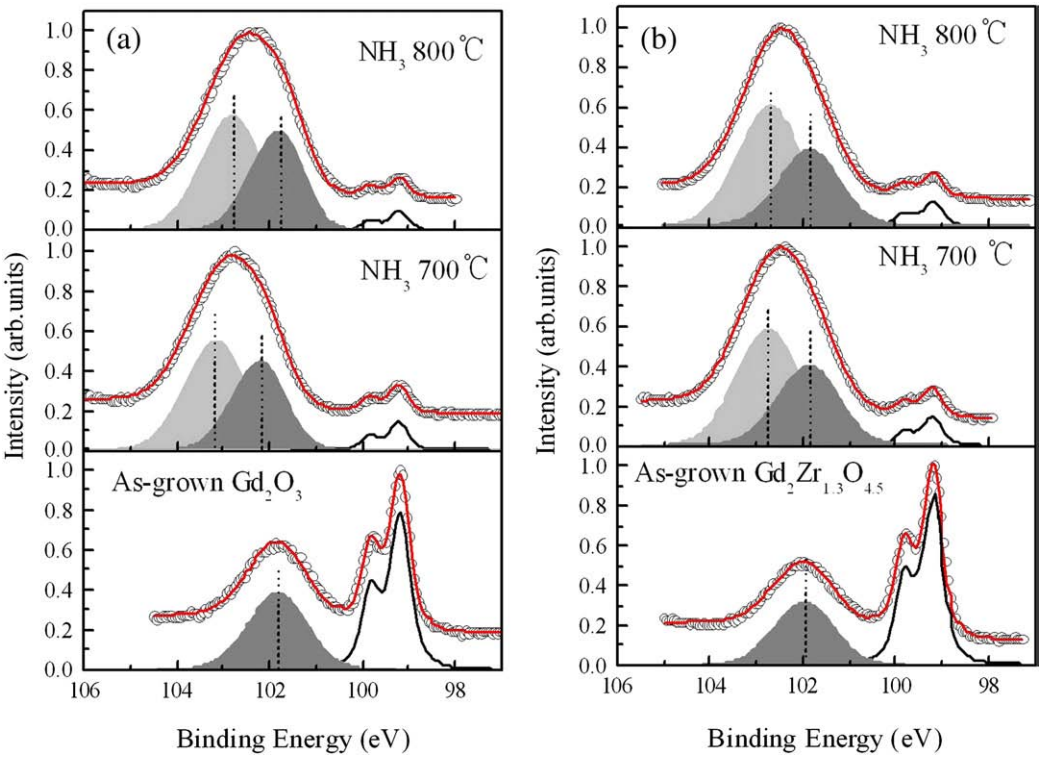

Fig. 4. Si 2p XPS spectra of (a) as-grown and nitrided Gd_2O_3 film (2 nm) in an ambient of NH_3 at 700 °C, 800 °C, and (b) as-grown and nitrided $Gd_2Zr_{1.3}O_{4.5}$ film (2 nm) in an ambient of NH_3 at 700 °C and 800 °C, respectively.

the peak intensity of the near 102 eV in a Zr-incorporated film is relatively small, compared to that without any Zr content, clearly indicating that the formation of the interfacial layer is suppressed in a film that contains Zr. After the nitridation process, the silicate peak and the dioxide peak become shifted toward lower binding energy due to the effect of N incorporation, and these peaks can be assigned to Si–N bonding and Si–O–N bonding, respectively [25]. Moreover, the increment of the silicate peak intensity with Zr content is also relatively small, while the peak at ~103 eV is much higher than that of the film without any Zr content. From these results, we can conclude that the crystalline structure is influenced by the interface state in close proximity to the substrate, as shown in Fig. 1(b) XRD spectra in the case of $Gd_{0.6}Zr_{1.9}O_{4.3}$. In comparing the molecular N_2 peaks, it appears that the generation of molecular N_2 was in proportion to the amount of N atoms that penetrated into the oxide film during the nitridation process. Some nitrogen atoms prefer to be bonded to Si, while others, which do not contribute to the reaction, easily form molecular N_2, due to the stable state of N_2. The peak position near 404 eV in Fig. 3 of the N1s XPS data indicates that molecular N_2 adsorbs weakly to Si near the interface, because the adsorbed peak position of N_2 is drastically shifted to a lower position, compared to that of N_2 in the gas phase [26].

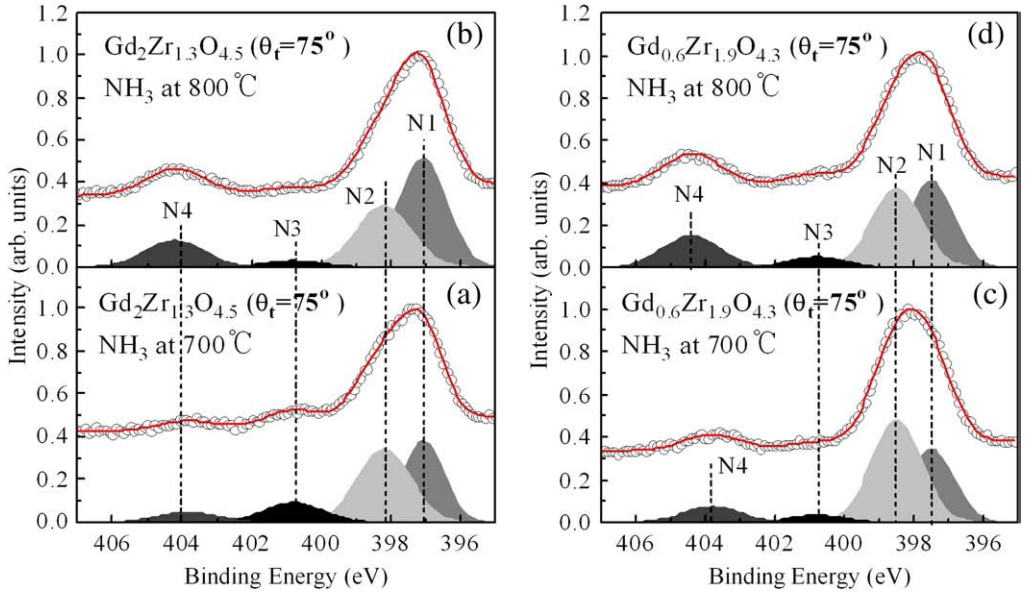

Fig. 5. N 1s XPS spectra (as shown in Fig 3 take-off angles 75°) of a $Gd_2Zr_{1.3}O_{4.5}$ film nitrided in an ambient of NH_3 at 700 °C (a), 800 °C (b), and a $Gd_{0.6}Zr_{1.9}O_{4.3}$ film nitrided in an ambient of NH_3 at 700 °C (c) and 800 °C (d), respectively.

To investigate the chemical states of nitrogen in Zr-incorporated Gd_2O_3 films in more detail, the XPS peak measured at a take-off angle of 75° was analyzed because of the nitrogen atoms that are primarily distributed at the interface between the oxide film and substrate. Fig. 5 shows N 1s spectra fitted to 4 peaks after a Shirley background subtraction for $Gd_2Zr_{1.3}O_{4.5}$ and $Gd_{0.6}Zr_{1.9}O_{4.3}$ films as a function of nitridation temperature. The positions of the N1, N2, N3, and N4 peaks are located at 397.5, 398.5, 401, and 404 eV. Each component can be assigned to a configuration as follows: N1 corresponds to NSi_3 with three Si nearest neighbors, N2 can be assigned to $N–(SiO_x)_3$, and N3 to $NSiO_2$ [27–29]. No Zr–N peak was observed in the N 1s spectrum, which is consistent with the Zr3d spectrum (not shown here). Thus, it can be concluded that most of the nitrogen is bonded directly to Si, which is consistent with the XPS data for Si 2p.

A similar tendency in peak intensity of N1 and N2 was found, regardless of the amount of Zr incorporated into Gd_2O_3; N1 increases relatively, while N2 decreases as the nitridation temperature increases from 700 °C to 800 °C. N atoms migrate more deeply into the interface when sufficient thermal energy is available to permit atomic rearrangement, resulting in an increase in the amount of N incorporated into the Si substrate for the formation of Si–N bonds at high temperature: i.e., N1 becomes increased with increasing annealing temperature [30]. The reported data show that the N4 state at 404 eV can be assigned to gaseous molecular [26]. The state was obviously increased at a high temperature of 800 °C in both the $Gd_2Zr_{1.3}O_{4.5}$ and $Gd_{0.6}Zr_{1.9}O_{4.3}$ films, indicating that as the amount of N atoms that diffuse into the film increases, the formation of molecular N_2 also increases. Thus, some N atoms are non-contributors to the formation of Si–N bonding with Si and contribute to the formation of molecular N_2. In addition, we observed that the molecular peaks disappear after thermal annealing at temperatures over 500 °C or after a few months of storage (not shown here). However, nitrogen atoms that are trapped at the internal interface retain their bonding because the Zr-silicate layer attracts nitrogen atoms. Therefore, the formation of a Zr-silicate layer at the interfacial region functions as a barrier layer in the film and enhances the thermal stability of the oxide film.

We measured O K-edge absorption spectra for Gd_2O_3 and $Gd_{0.6}Zr_{1.9}O_{4.3}$ films using NEXAFS because the O K-edge spectrum is very sensitive to the local structure of transition metal oxides. NEXAFS O K-edge data, as shown in Fig. 6, contains a resonance peak resulting from absorption by the lowest unoccupied molecular orbital which is correlated with π*anti-bonding. There are distinct separate sets of orbitals conventionally denoted by t_{2g} and e_g according their symmetry behavior in the absorption spectra (dotted line in Fig. 6(a)). The t_{2g} and e_g combinations of 2p oxygen can combine with metal d orbitals. Thus, the features of the two peaks are directly related to Gd 5d (Zr 4d) + O 2pπ and Gd 5d (Zr 4d) + O 2pσ, which appear as unoccupied hybridized orbitals [26,31]. Both as-grown Gd_2O_3 and the nitride-Gd_2O_3 film show a distorted peak that deviates from octahedral symmetry, which is caused by the formation of Gd-silicate at the interface. The Gd-silicate can be examined by XPS analysis of O 1s spectra (data not shown here). During the nitridation process, nitrogen atoms typically break oxygen bonds and substitute oxygen sites, which change the features of the absorption spectrum. On the other hand, a clear distinction between the peaks in the Zr-incorporated Gd_2O_3 film ($Gd_{0.6}Zr_{1.9}O_{4.3}$) is shown in Fig. 6(b). The energy separation between the lower t_{2g} and the higher e_g orbital indicates ligand–field splitting (△) in an octahedral symmetry, and their peak intensity ratio should represent a 3:2 in stoichiometry Gd_2O_3 and ZrO_2 [31]. In general, the mixing of e_g orbitals is larger than t_{2g}, because overlaps of the σ type are stronger than those of the π type. Thus, a d metal forms an anti-bonding state more strongly, resulting in e_g orbitals: i.e., a greater overlap interaction of these can increase octahedral ligand–field splitting. We observed this phenomenon in our spectra; the intensity of the e_g state and ligand–field splitting tends to increase gradually in proportion to the nitridation temperature used. Moreover, two peaks at higher energy are clearly apparent, corresponding to a_{1g} (Gd 6s (Zr 5s) + O 2p) and t_{1u} (Gd 6p (Zr 5p) + O 2p), respectively [26,31].

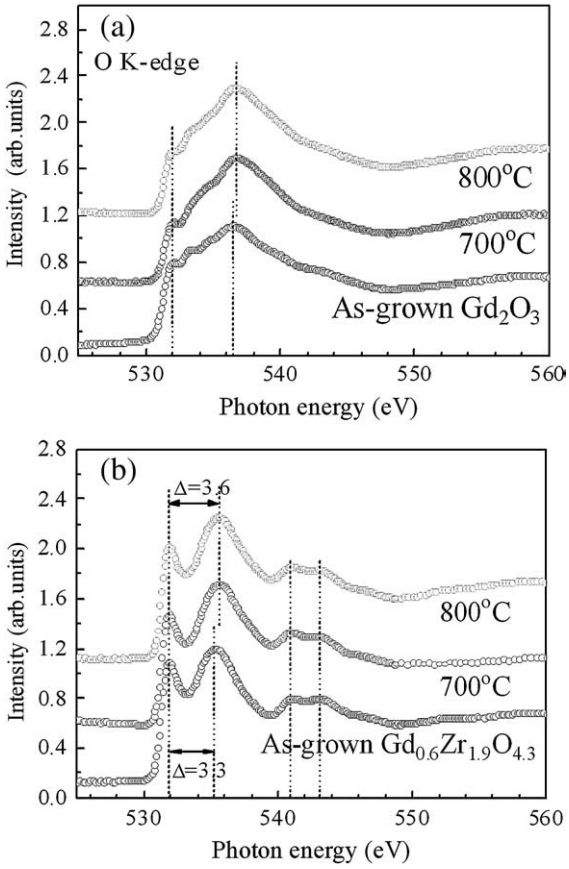

Fig. 6. Oxygen K-edge NEXAFS spectra for (a) as-grown and nitrided Gd_2O_3 films (30 nm) at 700 °C, 800 °C and (b) as-grown and nitrided $Gd_{0.6}Zr_{1.9}O_{4.3}$ films (30 nm) at 700 °C and 800 °C.

Pure Gd_2O_3 films without any Zr are not thermodynamically stable, while a Zr-incorporated Gd_2O_3 film forms a Zr-silicate and is very stable when in direct contact with Si. After the nitridation treatment, the Zr-incorporated Gd_2O_3 film largely maintains its symmetry and also maintains its crystal structure compared with a Gd_2O_3 film. A Gd_2O_3 film that contains incorporated Zr also attracts nitrogen atoms and nitridation at the interface creates a barrier layer that can suppress interfacial reactions between the film and the silicon substrate; i.e., this result is consistent with the XPS analysis in Fig. 4.

4. Conclusions

We investigated the physical properties of as-grown Gd_2O_3 and Zr-incorporated Gd_2O_3 films. Changes in the chemical bonding state during the nitridation process were investigated. An as-grown Gd_2O_3 film grown on Si (100) exhibits polycrystalline structure. The lattice constant of the film decreases with increasing amounts of incorporated Zr atoms, which has a significant effect, leading to changes in the crystalline structure of the film. In the case of a Gd_2O_3 film that contains large amounts of incorporated Zr, the phase of the $Gd_{0.6}Zr_{1.9}O_{4.3}$ changes from a cubic Gd_2O_3 to a monoclinic ZrO_2. Gd atoms react with silicon, resulting in the formation of a Gd-silicide layer at the interface between the Gd_2O_3 and Si substrate. However, the formation of the interfacial layer in the film can be controlled by the incorporation of Zr atoms and NH_3-nitridation. At high annealing temperatures, up to 800 °C, nitrogen atoms are largely distributed near the interface of a Zr-incorporated

Gd_2O_3 film: i.e., the incorporation of nitrogen into the interface is significantly dependent on the interfacial state. Silicon oxide terminals at the interface can attract nitrogen atoms. Moreover, nitrogen molecules are generated after the NH_3-nitridation process, the amounts of which are likely to be proportional to the content of Zr in the film and the annealing temperature used. Zr-incorporated Gd_2O_3 films exhibit good thermal stability and crystal quality.

Acknowledgments

This work was partly supported by the IT R&D program of MKE/IITA [2008-F-023-01] and a Seoul Science Fellowship from the Seoul Metropolitan Government.

References

[1] G.D. Wilk, R.M. Wallace, J.M. Anthony, J. Appl. Phys. 89 (2001) 5243.
[2] J. Aarik, A. Aidla, A.A. Kiisler, T. Uustare, V. Sammelselg, Thin Solid Films 340 (1999) 110.
[3] M. Copell, M. Gribelyuk, E. Gusev, Appl. Phys. Lett. 76 (2000) 436.
[4] R.D. Shannon, J. Appl. Phys. 73 (1993) 348.
[5] J. Kwo, M. Hong, A.R. Lortan, K.T. Queeney, Y.J. Chabal, J.P. Mannaerts, T. Boone, J.J. Krajewski, A.M. Sergent, J.M. Rosamilia, Appl. Phys. Lett. 77 (2000) 130.
[6] M. Hong, J. Kwo, A.R. Kortan, J.P. Mannaerts, A.M. Sergent, Science 283 (1999) 1897.
[7] I. Barin in collaboration with Gregor Platzki, Thermochemical data of pure substances. Vol. I, Weinheim, VCH, 1989, p. 758.
[8] T.S. Jeon, J.M. White, K.L. Kwong, Appl. Phys. Lett. 78 (2001) 368.
[9] J. Robertson, J. Vac. Sci. Technol., B 18 (2000) 1785.
[10] M.-H. Cho, D.W. Moon, S.A. Park, Y.S. Rho, Y.K. Kim, K. Jeong, C.H. Chang, J.H. Gu, J.H. Lee, S.Y. Choi, Appl. Phys. Lett. 84 (2004) 678.
[11] S.A. Park, Y.S. Roh, Y.K. Kim, J.H. Baeck, M. Noh, K. Jeong, M.-H. Cho, C.H. Chang, M.K. Joo, T.G. Kim, J.H. Song, D.-H. Ko, J. Appl. Phys. 98 (2005) 024906.
[12] S. Jeon, C.-J. Choi, T.-Y. Seong, H. Hwang, Appl. Phys. Lett. 79 (2002) 245.
[13] Y.-S. Lin, R. Puthenkovilakam, J.P. Chang, C. Bouldin, I. Levin, N.V. Nguyen, J. Ehrstein, Y. Sun, P. Pianetta, T. Conard, W. Vandervorst, V. Venturo, S. Selbrede, J. Appl. Phys. 93 (2003) 5945.
[14] T. Ito, T. Nakamura, H. Ishikawa, J. Electrochem. Soc. 129 (1982) 184.
[15] G.J. Dunn, J. Appl. Phys. 65 (1989) 4879.
[16] W. Kern, RCA Rev. 31 (1970) 234.
[17] Jonathan S. Morrell, Ziling B. Xue, Eliot D. Specht, Amit Goyal, Patrick M. Martin, Dominic F. Lee, R. Feenstra, D.T. Verebelyi, D.K. Christen, Thomas G. Chirayil, Mariappan Paranthaman, Catherine E. Vallet, David B. Beach, J. Mater. Res. 15 (2000) 621.
[18] M. Hong, Z.H. Lu, J. Kwo, A.R. Kortan, J.P. Mannaerts, J.J. Krajewski, K.C. Hsieh, L.J. Chou, K.Y. Cheng, Appl. Phys. Lett. 76 (2000) 312.
[19] I. Gerocs, G. Molnar, E. Jaroli, E. Zsoldos, G. Peto, J. Gyulai, E. Bugiel, Appl. Phys. Lett. 51 (1987) 2144.
[20] J.C. Chen, G.H. Shen, L.J. Chen, J. Appl. Phys. 84 (1998) 6083.
[21] Ulrich Muller, Inorganic Structural Chemistry, John Wiley & Sons, New York, 1993, p. 210.
[22] C. Zhao1, G. Roebben, M. Heyns, O. Van Der Biest, Key Eng. Mater. 206 (2002) 1285.
[23] F. Tcheliebou, M. Boulouz, A. Boyer, J. Mater. Res. 12 (1997) 3260.
[24] N. Yabumoto, K. Minegishi, Y. Komine, K. Saito, Jpn. J. Appl. Phys. 29 (1990) L490.
[25] F.N. Cubaynes, V.C. Venezia, C. van der Marel, J.H.M. Snijders, J.L. Everaert, X. Shi, A. Rothschild, M. Schaekers, Appl. Phys. Lett. 86 (2005) 172903.
[26] M.-H. Cho, K.B. Chung, C.N. Whang, D.-H. Ko, J.H. Lee, N.I. Lee, Appl. Phys. Lett. 88 (2006) 202902.
[27] J.P. Chang, M.L. Green, V.M. Donnelly, R.L. Opila, J. Eng Jr., J. Sapjeta, P.J. Silverman, B. Weir, H.C. Lu, T. Gustafsson, E. Garfunkel, J. Appl. Phys. 87 (2000) 4449.
[28] J.R. Shallenberger, D.A. Cole, S.W. Novak, J. Vac. Sci. Technol., A 17 (1999) 1086.
[29] M.-H. Cho, K.B. Chung, D.-W. Moon, Appl. Phys. Lett. 89 (2006) 182908.
[30] Masao Takahashi, Toshiko Mizokuro, Yasushiro Nishioka, Hikaru Kobayashi, Surf. Sci. 518 (2002) 72.
[31] J.G. Chen, Surf. Sci. Rep. 30 (1997) 1.